Human Molecular Genetics, 2007, Vol. 16, No. 24 ***3136–3148***
doi:10.1093/hmg/ddm275
Advance Access published on September 19, 2007

Succinate inhibition of α-ketoglutarate-dependent enzymes in a yeast model of paraganglioma

Emily H. Smith, Ralf Janknecht and L. James Maher III*

Department of Biochemistry and Molecular Biology, Mayo Clinic College of Medicine, 200 First Street, SW, Rochester, MN 55905, USA

Received August 8, 2007; Revised and Accepted September 14, 2007

The tricarboxylic acid (TCA) cycle enzyme succinate dehydrogenase (SDH) is a tumor suppressor. Heterozygosity for defective SDH subunit genes predisposes to familial paraganglioma (PGL) or pheochromocytoma (PHEO). Models invoking reactive oxygen species (ROS) or succinate accumulation have been proposed to explain the link between TCA cycle dysfunction and oncogenesis. Here we study the biochemical consequences of a common familial PGL-linked mutation, loss of the SDHB subunit, in a yeast model. This strain has increased ROS production but no evidence of mutagenic DNA damage. Because the strain lacks SDH activity, succinate accumulates dramatically and inhibits α-ketoglutarate (αKG)-dependent enzyme Jlp1, involved in sulfur metabolism, and αKG-dependent histone demethylase Jhd1. We show that mammalian JmjC-domain histone demethylases are also vulnerable to succinate inhibition *in vitro* and in cultured cells. Our results suggest that any αKG-dependent enzyme is a potential target of accumulated succinate in oncogenesis. The possible role that inhibition of these enzymes by succinate may have in oncogenesis is discussed.

INTRODUCTION

Mitochondrial complex II (succinate dehydrogenase, SDH) contains four nuclear-encoded subunits (SDHA-D) localized to the inner mitochondrial membrane. The SDHA subunit catalyzes the oxidation of succinate to fumarate in the tricarboxylic acid (TCA) cycle. The resulting electrons are passed through the iron-sulfur clusters of SDHB, which is anchored to the inner mitochondrial membrane by SDHC and SDHD subunits. Electrons ultimately flow to the ubiquinone pool of the electron transport chain (ETC) to generate ATP. Mutations in genes encoding SDH subunits have been linked to severe encephalopathy and, more recently, to familial paraganglioma (PGL) and pheochromocytoma (PHEO) (PHEO: adrenal gland PGL). Mutations affecting SDHA are rare and associated with Leigh Syndrome, a neurological disorder typical of mitochondrial ETC defects (1). In contrast, mutations in genes encoding SDHB, C, and D predispose carriers to familial PGL and PHEO in an autosomal dominant fashion (2–4). A broad spectrum of SDH mutations has been reported in familial PGL. This range of mutations suggests that loss of function of SDH subunits SDHB, SDHC, or SDHD is the common predisposing factor in familial PGL.

Two plausible hypotheses have been proposed to explain the peculiar linkage between disruption of electron flow through mitochondrial complex II and tumorigenesis in neuroendocrine cells (Fig. 1). In the reactive oxygen species (ROS) hypothesis (Fig. 1A), it is proposed that an intact, catalytically active SDHA subunit generates genotoxic ROS by uncoupled electron flow from succinate to oxygen or water in cells where one of the electron-carrying subunits (SDHB, SDHC or SDHD) is missing or inactive (5,6). The ROS model implies that genotoxic ROS mutagenize nuclear proto-oncogenes or tumor suppressors. This model predicts that ROS should be increased in cells lacking SDHB, SDHC or SDHD, but not when SDHA is missing. Although certain mutations in these genes result in ROS production in *Caenorhabditis elegans*, *Saccharomyces cerevisiae* and mammalian cell lines (5–8), it is not clear that ROS accumulate to levels that are mutagenic.

*To whom correspondence should be addressed. Tel: +1 5072849041; Fax: +1 5072842053; Email: maher@mayo.edu (J.M.)

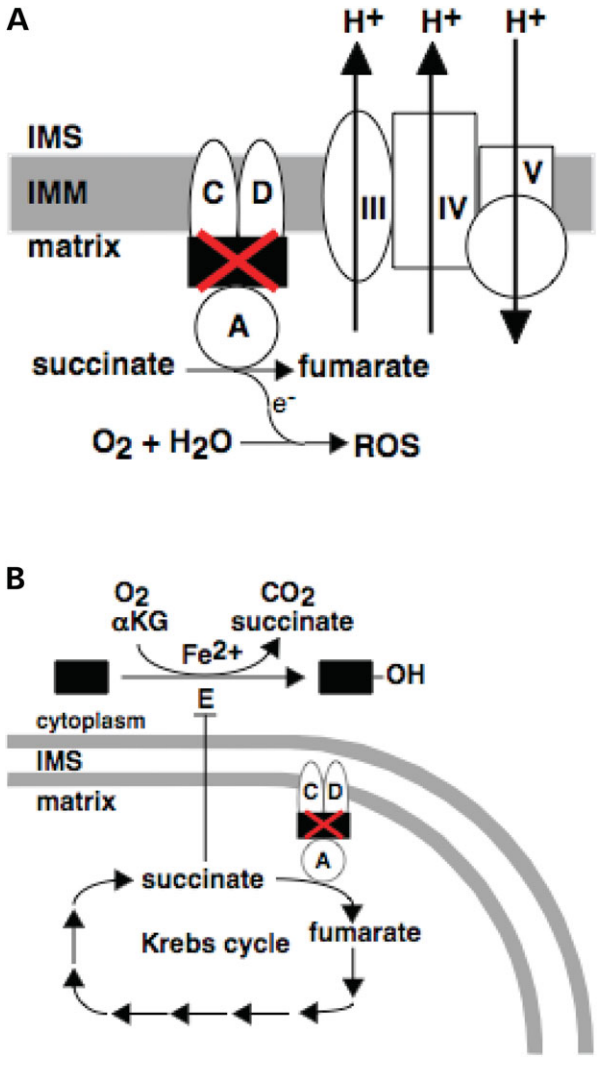

Figure 1. Two models for the origin of human familial PGL resulting from loss of SDHB. (**A**) ROS model. The loss of SDHB results in release of an uncoupled, catalytically active SDHA subunit that oxidizes succinate but passes electrons inappropriately to oxygen or water to generate ROS. (**B**) Succinate accumulation model. The loss of SDHB results in loss of SDH activity and causes succinate accumulation. Excess succinate is shuttled from the mitochondrial matrix to the cytoplasm, where it inhibits any of several αKG-dependent enzymes **(**E**)** that regulate levels or activities of important regulatory proteins (black box). IMS, inner membrane space; IMM, inner mitochondrial membrane.

In the succinate accumulation hypothesis (Fig. 1B), loss or inactivation of SDHB, C or D proteins yields a catalytically inactive SDHA subunit, resulting in blockade of the TCA cycle and diffusion of accumulated succinate to the cytoplasm. Succinate can then act as an inhibitor of α-ketoglutarate (αKG)-dependent enzymes that use ferrous iron and molecular oxygen as cofactors to hydroxylate their substrates and generate succinate as a product (9–11). It has been demonstrated that two such αKG-dependent enzymes, the prolyl hydroxylases EglN1 and EglN3, are inhibited by succinate accumulation in cells that have lost SDHD function (9,11). EglN1 and EglN3 are involved in the regulation of HIF-1α and c-Jun-dependent apoptosis, respectively. Inhibition of EglN1 by succinate results in stabilization of the oxygen-sensing transcription factor, HIF-1α, even when adequate oxygen is present (11). Inhibition of EglN3 has been hypothesized to prevent normal neuronal cell culling by blocking c-Jun-dependent apoptosis during development (9).

Enzymes subject to succinate inhibition are not limited to EglN1 and EglN3. Other αKG-dependent enzyme superfamily members have also recently been identified and implicated in cancer. For example, p53 induces the αKG-dependent enzyme, alpha(II) collagen prolyl-4-hydroxylase, resulting in anti-angiogenic collagen fragments (12). In addition, human JmjC-domain histone demethylases (JHDMs) are part of the αKG-dependent enzyme superfamily by virtue of the JmjC domain (13). Recently, five JmjC-domain-containing ORFs in *S. cerevisiae* were identified and four were characterized as true αKG-dependent histone demethylases (14). Multiple αKG-dependent histone demethylases may participate in epigenetic regulation of oncogenes and tumor suppressor genes. Enzymes of this superfamily are potential targets for inhibition by succinate accumulation.

To evaluate the ROS and succinate accumulation hypotheses in a genetically and biochemically tractable system, we characterized an *S. cerevisiae* strain lacking Sdh2 (the yeast ortholog of mammalian SDHB) as a model of a typical familial PGL mutation. We report that yeast cells disrupted in *SDH2* (*sdh2*Δ) show increases in ROS production and protein oxidation but no detectable increase in DNA damage. More strikingly, *sdh2*Δ cells dramatically accumulate succinate resulting in inhibition of at least two αKG-dependent enzymes that generate succinate as a by-product. One of these enzymes is an αKG-dependent JHDM. We show that a corresponding human JHDM is susceptible to succinate inhibition, both as a purified enzyme and when expressed in mammalian cells. Inhibition of JHDMs has the potential to derange epigenetic regulation of growth control genes. These results strongly support the succinate accumulation hypothesis of familial PGL causation by SDH mutations. Moreover, these results emphasize that αKG-dependent enzyme targets other than mammalian EglN1 and EglN3 may be important in understanding how a TCA cycle enzyme functions as a tumor suppressor in neuroendocrine cells.

RESULTS

ROS production in cells lacking *SDH2*

According to the ROS hypothesis, loss-of-function *SDHB* mutations disrupt complex II without affecting SDHA catalysis. This hypothesis predicts that yeast Sdh1 (yeast ortholog of mammalian SDHA) should persist in the absence of Sdh2. Because no commercial antibody against yeast Sdh1 was available, we modified the chromosomal copy of *SDH1* in yeast so that Sdh1 was C-terminally tagged with GFP to allow its detection by western blotting and microscopy. To demonstrate that the GFP tag did not interfere with Sdh1 function, the growth of cells expressing GFP-tagged Sdh1 was compared with wild-type (WT) cells on different carbon sources. Yeast cells supplemented with a fermentable carbon source such as glucose survive by glycolysis. In contrast,

yeast grown on a non-fermentable carbon source such as glycerol requires a functional ETC. WT, Sdh1-GFP (WT*) and *sdh1*Δ cells grew equally on glucose (Fig. 2A). We found that cells producing GFP-tagged Sdh1 grew almost as rapidly as WT cells on glycerol, whereas *sdh1*Δ cells grew slowly under these conditions (Fig. 2A). This result shows that the GFP tag does not inactivate Sdh1.

We created *sdh2*Δ cells carrying the chromosomal *SDH1-GFP* gene (*sdh2*Δ*). Western blotting and fluorescence microscopy showed that, like WT* cells, *sdh2*Δ* cells produce Sdh1-GFP that is localized to mitochondria (Fig. 2B and C). This persistence of Sdh1 in the absence of Sdh2 meets one prediction of the ROS hypothesis. We performed several experiments to determine if deletion of *SDH2* indeed leads to ROS generation in yeast. It has previously been shown that inhibition of Complex III in the ETC by antimycin A causes a 3-fold increase in superoxide production in *S. cerevisiae* as determined by fluorescence detection of dihydroethidine (DHE) oxidation to ethidium (15). Interestingly, we observed that the *sdh2*Δ strain produced elevated levels of superoxide comparable to yeast treated with antimycin A, consistent with the ROS hypothesis (Fig. 3A and B). However, we found that superoxide levels were also increased in *sdh1*Δ cells. This result shows that SDH disruptions can induce ROS, but it is not consistent with an ROS model that invokes a functional but uncoupled catalytic Sdh1 subunit as the ROS source.

It has been demonstrated that loss of superoxide dismutase1 (*sod1*Δ*)* results in increased sensitivity to oxidative stress in yeast (16). We found that *sdh2*Δ cells were sensitized to hydrogen peroxide to an extent comparable to an *sod1*Δ mutant (Fig. 3C). Slow growth on non-fermentable ethanol due to oxidative stress could be modestly ameliorated with antioxidant treatment, as seen with *sod1*Δ cells (Fig. 3D). The slow growth phenotype of *sdh2*Δ cells on ethanol medium appears to be due to both oxidative stress and the inefficient utilization of the non-fermentable carbon source (non-functional TCA cycle). Slow growth caused by inability to metabolize EtOH cannot be reversed with antioxidants. However, the small contribution of oxidative stress to the slow growth phenotype of *sdh2*Δ cells on YPE was revealed by modest growth improvement upon antioxidant treatment (Fig. 3D). We conclude that *sdh2*Δ cells accumulate superoxide to levels that cause hypersensitivity to H_2O_2 and that antioxidants can improve growth of *sdh2*Δ cells. In this respect, the behaviors of *sdh2*Δ and *sod1*Δ cells are surprisingly similar.

Significance of induced ROS in SDH mutant yeast

If superoxide is mutagenic in *sdh2*Δ cells, DNA and proteins should show evidence of oxidative damage. Superoxide radicals can react with cellular iron via Fenton chemistry to produce extremely reactive hydroxyl radicals and other ROS (17). These species oxidize proteins and damage DNA with the potential to generate oncogenic mutations. The absence of SDH subunits resulted in a 3–4-fold increase in superoxide production relative to WT yeast (Fig. 3B). To determine the toxicity of superoxide produced in *sdh2*Δ cells, protein oxidation and DNA damage were assessed. A western blot was performed to monitor accumulation of carbonyl groups in proteins as a marker of oxidative damage. Protein oxidation was increased in *sdh2*Δ cells relative to WT cells (Fig. 4A). The increase in protein oxidation was comparable to that observed in *sod2*Δ cells (Fig. 4A).

Nuclear DNA vulnerability to mutagenesis in the presence of *SDH* mutations was previously assessed in a genome-wide screen of the BY4741 deletion strain library (18). Mutation frequency was assayed by measuring the rate of spontaneous reversion mutagenesis for several marker genes. The role of *sod1* in genomic stability has been well documented (19–21). An *sod1*Δ strain was found to have a mutator phenotype in this assay with a spontaneous mutation rate comparable to strains deleted in DNA repair genes, *rad5*Δ and *msh6*Δ (18). In contrast, the spontaneous mutation frequency in the *sdh2*Δ mutant was reported to be similar to WT cells, demonstrating that enhanced ROS production in *sdh2*Δ cells does not detectably increase the rate of nuclear DNA mutations.

Although there is no evidence to suggest enhanced mutagenesis of nuclear DNA in *sdh2*Δ mutants, dysfunctional complex II is likely to produce the highest ROS concentrations locally in the mitochondria. We therefore tested if mtDNA experiences oxidative damage in the *sdh2Δ* strain. We used quantitative PCR to amplify a 6.9 kbp segment of the mitochondrial *COX1* gene in an assessment of mtDNA damage (22). Oxidative DNA lesions inhibit DNA polymerase. The level of oxidative damage can be estimated by comparing the rate of 6.9 kbp template amplification relative to amplification of a 298 bp reference region of *COX1*. Amplification of the short *COX1* segment controls for mitochondrial genome copy number because of the low probability of an oxidative lesion within such a small target. Whereas hydrogen peroxide caused detectable mitochondrial DNA damage in WT cells (Fig. 4B), levels of endogenous ROS in *sdh1*Δ, *sdh2*Δ and *sod1*Δ cells were insufficient to cause detectable mitochondrial DNA damage (Fig. 4B). Although based upon a relatively insensitive assay, this result suggests that endogenous ROS damage to mtDNA in yeast cells with SDH gene disruptions does not exceed the level in *sod1*Δ cells. Combined with previous genetic evidence that SDH gene disruption does not produce a mutator phenotype (18), this result argues against acute genotoxicity by ROS in SDH mutant yeast.

We further analyzed yeast strains for evidence of signaling in response to oxidative stress. Yeast transcription factor yAP-1 is activated by oxidative stress, providing a biosensor for the level of superoxide generated in *sdh2*Δ cells (23). A plasmid with a *lacZ* reporter gene under the control of yAP-1 binding sites was tested in WT, *sdh1*Δ and *sdh2*Δ strains. The reporter responded equally to hydrogen peroxide treatment in each strain, and there was no difference in basal yAP-1 activation (Table 1). These results confirm that the increased ROS detected by sensitive assays in *sdh1*Δ and *sdh2*Δ cells are not inducing detectable DNA damage or an oxidative stress response in yeast.

Succinate accumulation upon SDH disruption

According to the succinate accumulation hypothesis of PGL origin, loss of *SDHB* results in loss of SDH activity and subsequent succinate accumulation inhibits αKG-dependent

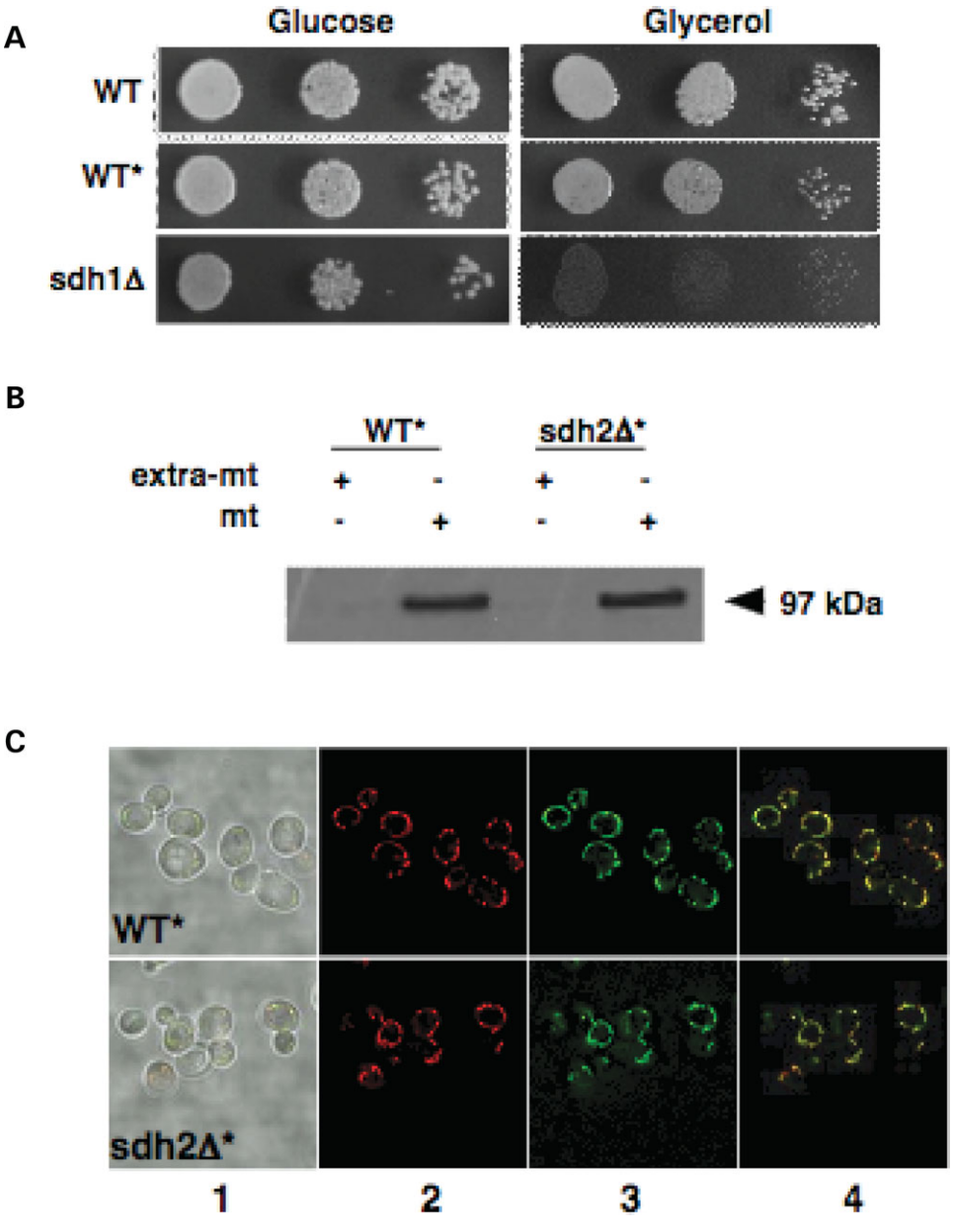

Figure 2. Sdh1 is present in the absence of Sdh2. (**A**) GFP-tagged Sdh1 is functional. Ten-fold serial dilutions of the indicated yeast strains grown on media with glucose or glycerol as the only carbon source. Yeast strains producing GFP-tagged Sdh1 are indicated (asterisk). (**B**) Western blot for GFP-tagged Sdh1 showing the presence of Sdh1 in *sdh2*Δ cells. Extra-mt: extra-mitochondrial extract; mt: mitochondrial extract. (**C**) WT* and *sdh2*Δ* cells (panel 1) are stained with tetramethylrhodamine to indicate mitochondria (panel 2) or excited at 470 nm to visualize GFP fluorescence at 525 nm (panel 3). Panel 4 shows the overlay of panels 2 and 3.

enzymes such as EglN1 and EglN3 (Fig. 1B). We tested the succinate accumulation hypothesis in yeast by first analyzing the activities of ETC components. We found that neither *sdh1*Δ, nor s*dh2*Δ cells have measurable SDH activity (Supplementary Material, Table S1). This result confirms that although Sdh1 is stable in the absence of Sdh2 (Fig. 2), the persisting Sdh1 is not enzymatically active. Furthermore, complex II+III activity was completely abolished in both SDH mutants without a corresponding compensation in NADH dehydrogenase activity (Supplementary Material, Table S1). As a result, complex IV activity was decreased in the SDH mutants (Supplementary Material, Table S1). Disruption of complex II activity should alter TCA cycle metabolite levels in the mitochondrial matrix. Indeed, gas chromatography/mass spectrometry (GC/MS) analysis of yeast lysates revealed that succinate accumulates to 8-fold higher levels in *sdh2*Δ cells relative to WT cells (Fig. 5, Supplementary Material, Table S2). Fumarate and malate levels are reduced at least 50-fold, whereas citrate and aconitate are not affected (Fig. 5). αKG extracted from both WT and *sdh2*Δ cells was below the level of detection for this sensitive assay.

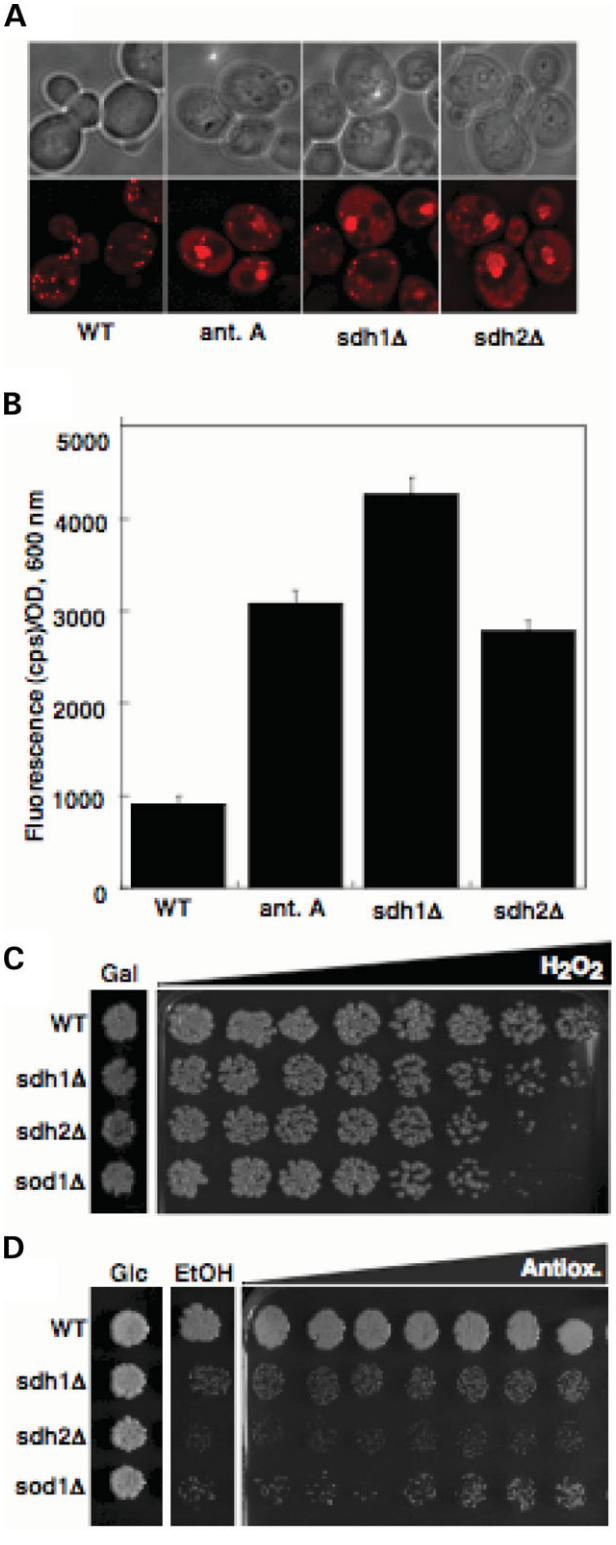

Figure 3. ROS in *sdh2*Δ yeast cells. (**A** and **B**) Measurement of superoxide. The presence of superoxide radicals was probed with DHE in WT with or without antimycin A (ant. A), *sdh1*Δ and *sdh2*Δ yeast strains by microscopy (A) and independently by fluorometry where data are represented as mean ± SEM (B). (**C** and **D**) Superoxide sensitivity. Equal samples of the indicated yeast strains were grown on media with an increasing gradient of hydrogen peroxide in galactose (Gal) medium (C) or antioxidant in ethanol (EtOH) medium (D). Cells grown in glucose (Glc) are shown for comparison.

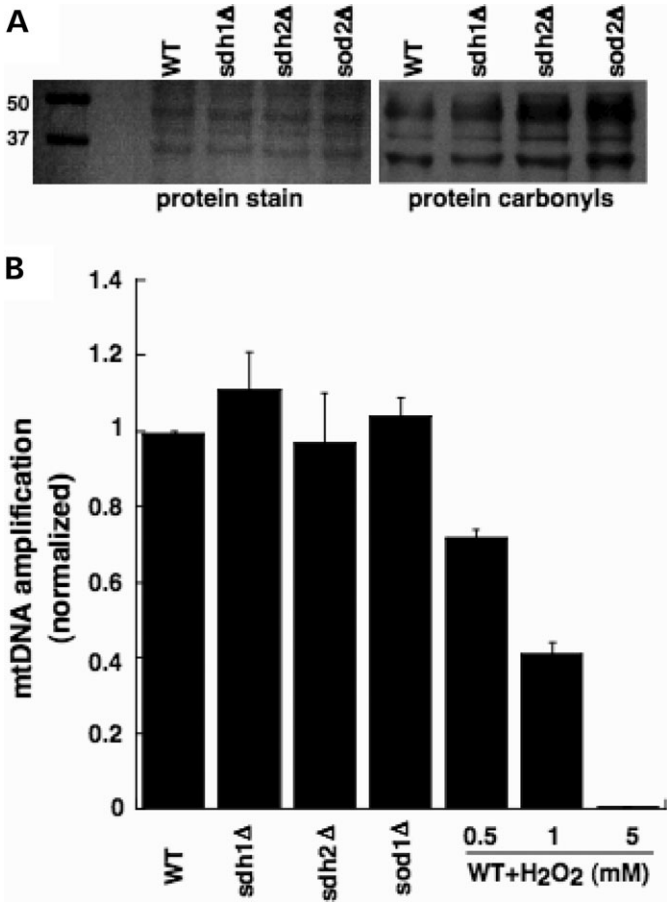

Figure 4. Effect of ROS on macromolecules. (**A**) Protein oxidation by western blot. *Left*: equal protein loading shown by Amido black stain. *Right*: protein carbonyl detection. (**B**) Damage assessment of mtDNA by QPCR. 6.9 kbp mtDNA product abundance normalized to 298 bp mtDNA product abundance for WT, *sdh1*Δ, *sdh2*Δ and *sod1*Δ cells as well as WT cells treated with increasing concentrations of H_2O_2. Data are represented as mean ± SEM.

Table 1. ROS signaling in SDH mutant yeast[a]

	WT	*sdh1* Δ	*sdh2* Δ
Basal	14.7 ± 1.5	15.7 ± 4.5	16.0 ± 2.6
Induced (100 μM H_2O_2)	47.7 ± 7.4	49.0 ± 3.6	54.3 ± 18.9

[a]β-Galactosidase reporter activity from yAP-1-driven reporter plasmid in Miller units.

EglN1 and EglN3 enzymes have been suggested as targets of inhibition by succinate accumulation in SDH-deficient mammalian cell lines. Other members of the αKG-dependent enzyme superfamily should also be susceptible to inhibition by succinate accumulation. We tested this hypothesis by studying αKG-dependent yeast enzymes. *Saccharomyces cerevisiae* encodes a sulfur-scavenging pathway that requires the function of an αKG-dependent enzyme, Jlp1, when sulfonate esters such as isethionate replace sulfate as the only sulfur source [Fig. 6A (24)]. WT, *jlp1*Δ and *sdh2*Δ cells grew

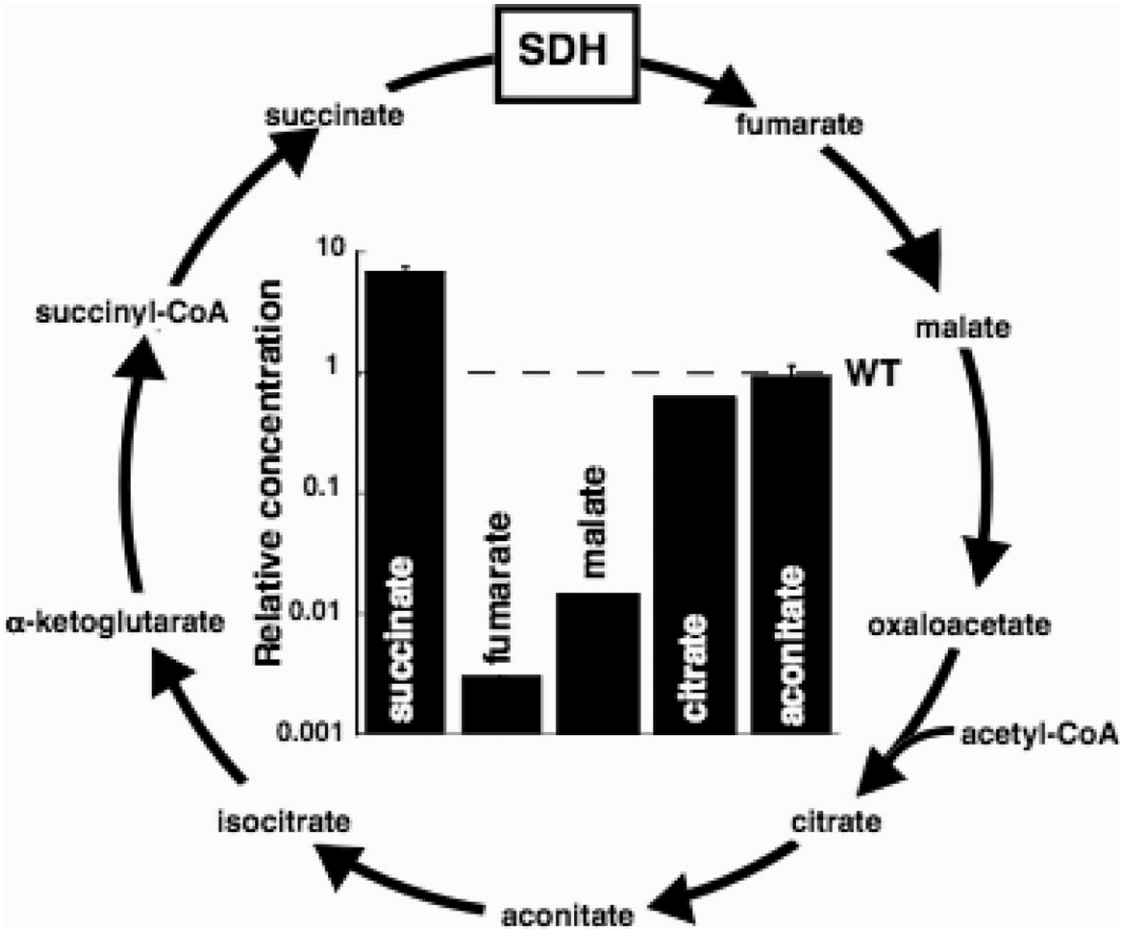

Figure 5. Krebs cycle metabolite levels in yeast strains. Succinate, fumarate, malate, citrate and aconitate levels were measured by GC/MS analysis of whole cell lysates for WT and *sdh2*Δ strains grown to log phase. Data are represented as the mean ± SEM of μg metabolite/mg total protein extract for *sdh2*Δ yeast normalized to the corresponding WT value.

equally well in the presence of ammonium sulfate (Fig. 6B). In contrast, when isethionate was the only sulfur source, both *jlp1*Δ and *sdh2*Δ cells grew slowly (Fig. 6C). This result is consistent with Jlp1 poisoning by succinate accumulation in the *sdh2*Δ strain. We found that WT cells were not poisoned by exogenous succinate if ammonium sulfate was the only sulfur source (Fig. 6D). However, growth of WT cells was strongly inhibited by exogenous succinate when isethionate was the only sulfur source (Fig. 6E). We hypothesized that repression of Jlp1 function by exogenous succinate was a result of product inhibition, suggesting that increasing the concentration of Jlp1 co-substrate αKG could shift the equilibrium in favor of isethionate catabolism. Remarkably, succinate poisoning of Jlp1 enzyme activity in WT cells was indeed rescued by treatment with αKG (Fig. 6E).

In addition to the sulfur-scavenging enzyme, Jlp1, *S. cerevisiae* also encodes a histone demethylase, Jhd1, that belongs to the JmjC-domain-containing histone demethylase (JHDM) class. Jhd1 is an αKG-dependent enzyme by virtue of its JmjC domain. The JmjC domain is predicted to fold into an eight β-sheet 'jellyroll' structure that contains highly conserved residues essential for catalytic activity (13,25). Jhd1 is orthologous to mammalian JHDMs whose histone substrate specificity is conferred by non-catalytic residues in the JmjC domain and flanking domains. Both yeast and mammalian αKG-dependent JHDMs should be susceptible to inhibition by succinate accumulation (product inhibition). It has been reported that yeast *SET2* encodes a histone H3 lysine36 (H3-K36) methylase and disruption of *SET2* results in the complete absence of H3-K36 methylation (26). Yeast Jhd1 specifically demethylates dimethylated H3-K36 (H3-K36me2) [Fig. 7A (27)]. We hypothesized that loss of the H3-K36 demethylase Jhd1 or inhibition of Jhd1 by succinate in *sdh2*Δ cells should therefore cause accumulation of H3-K36me2. Indeed, we found that both *jhd1*Δ and *sdh2*Δ cells showed an increase in H3-K36me2 relative to WT cells (Fig. 7B). We hypothesized that treatment of WT cells with exogenous succinate and/or αKG would affect the extent of H3-K36 methylation. We found by western blot that WT cells treated with exogenous succinate increased H3-K36me2 levels and that co-treatment with αKG showed the detectable (though subtle) ability to partially reverse this effect (Fig. 7C).

To extend this evidence for succinate inhibition of JHDM activity, we monitored the *in vitro* histone demethylase activity of human histone demethylase JMJD2D (a JHDM3 family member). JMJD2D specifically demethylates trimethy-

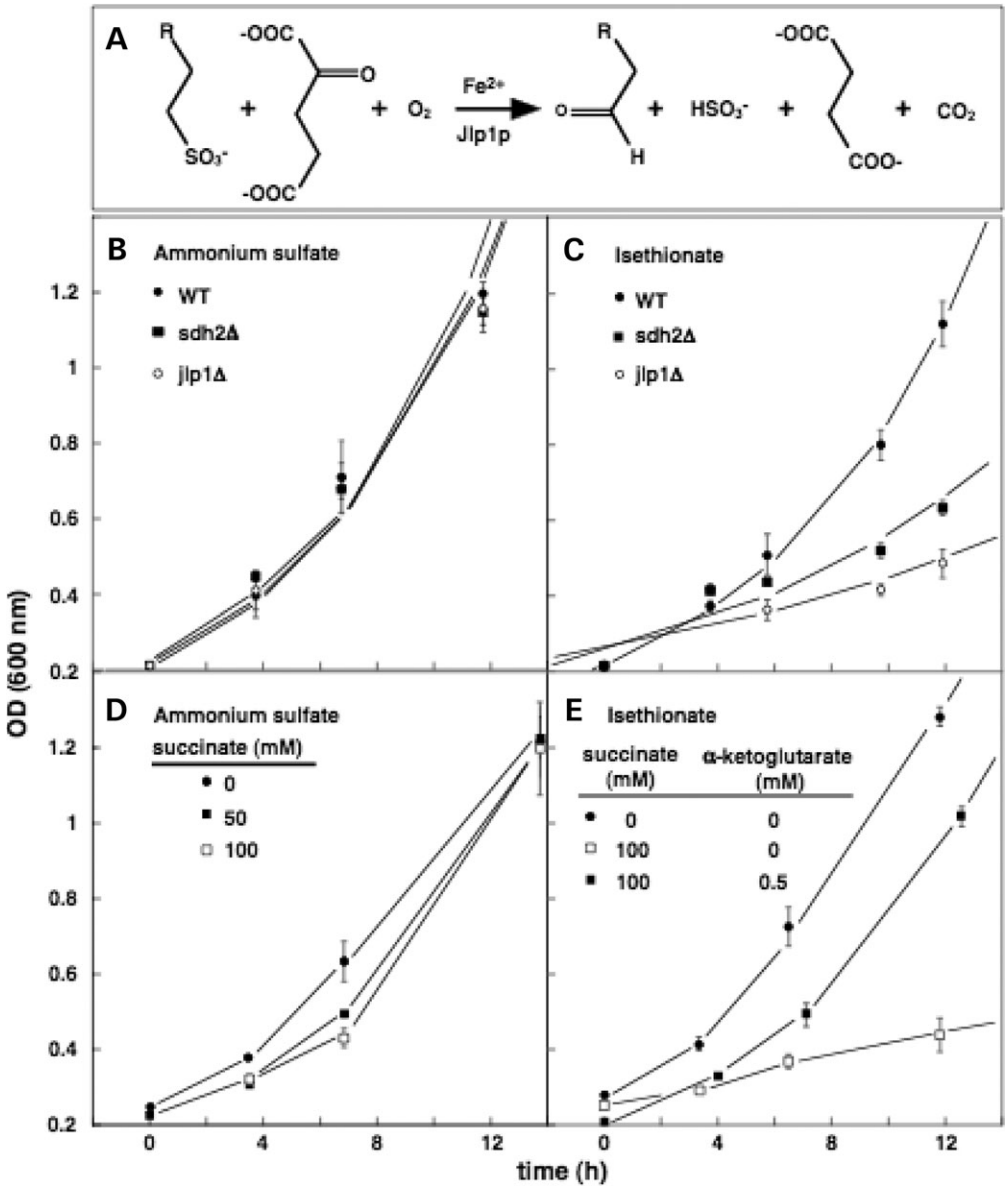

Figure 6. Succinate accumulation in the *sdh2Δ* mutant inhibits the αKG-dependent enzyme Jlp1. (**A**) Oxidative metabolism of sulfonate esters by Jlp1. (**B** and **C**) Comparison of yeast growth in ammonium sulfate minimal media (B) or isethionate minimal media (C). (**D** and **E**) Comparison of WT yeast growth in ammonium sulfate minimal media supplemented with succinate (D) or isethionate minimal media supplemented with the indicated combinations of succinate and/or αKG (E). Data in (B–E) are represented as mean ± SEM.

lated histone H3 lysine 9 (H3-K9me3) (13). We confirmed the *in vitro* histone demethylase activity was specific to the purified JmjC domain by showing complete absence of H3-K9me3 demethylase activity in an H192A mutant that abolishes the iron binding capacity of the JmjC domain (Fig. 7D, lanes 1–3). On the basis of our observations for yeast Jhd1 *in vivo*, we predicted that increasing concentrations of succinate would inhibit the purified human JMJD2D enzyme. We confirmed JMJD2D inhibition by 1–10 mM succinate (Fig. 7D, lanes 3–5). Succinate inhibition could be relieved with increasing concentrations of αKG, as expected (Fig. 7D, lanes 5–8).

We next studied the effect of succinate on mammalian histone demethylases *in vivo* by treating cultured T293 cells with the membrane-permeable dimethyl ester form of succinate, dimethylsuccinate (DMS) that has previously been used to cause intracellular succinate accumulation (11). We found that overexpression of JMJD2D specifically demethylates H3-K9me3 residues and that treatment with DMS inhibits this effect (Fig. 7E). These results formally open the possibility that succinate poisoning of histone demethylases could alter gene expression by an epigenetic mechanism.

DISCUSSION

SDH mutations predisposing to human familial PGL are frequently loss-of-function alleles due to protein truncation by

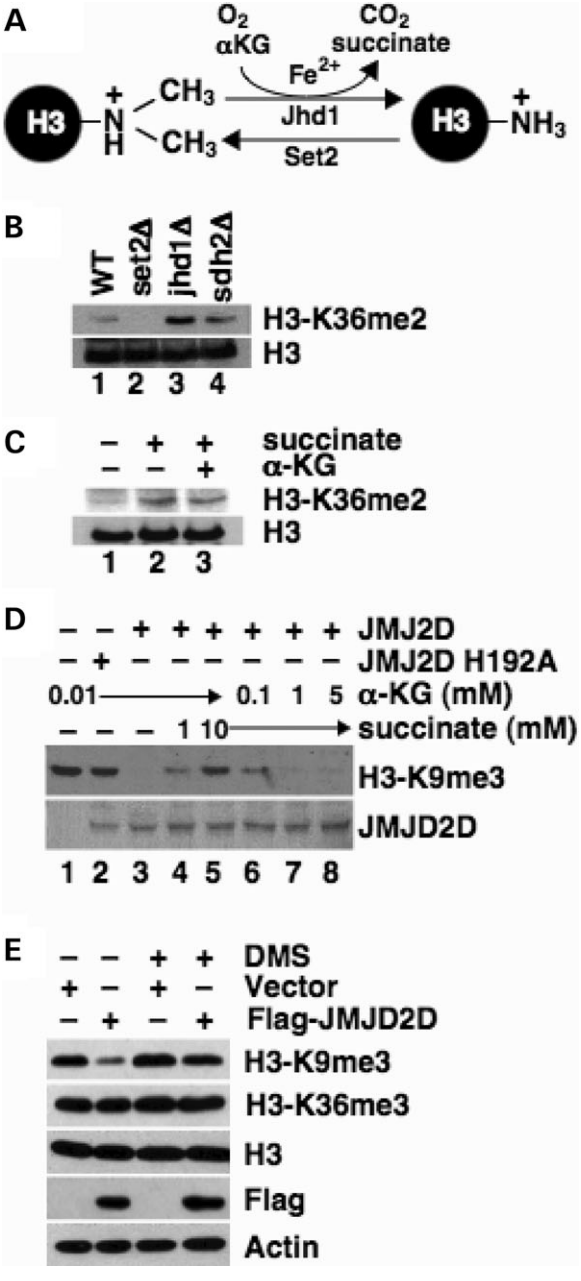

Figure 7. Succinate accumulation inhibits yeast and human enzymes. (**A**) Demethylase reaction mechanism of Jhd1. (**B**) Comparison of H3-K36me2 abundance by western blotting in WT, *set2*Δ, *jhd1*Δ and *sdh2*Δ yeast strains. Histone H3 (H3), loading control. (**C**) Comparison of H3-K36me2 abundance by western blotting in WT yeast cells treated with 50 mM succinate and/or 1 mM αKG. (**D**) Comparison of *in vitro* human JMJD2D WT and H192A mutant histone demethylase activities (lanes 1–3) in the presence of 0–10 mM succinate (lanes 3–5) followed by increasing concentrations of αKG in the presence of 10 mM succinate (lanes 5–8). Lane 1 shows reaction without enzyme. (**E**) Comparison of human JMJD2D histone demethylase activity in cultured cells in the absence or presence of 100 mM DMS.

premature nonsense codons. Mutational 'hot spots' are not observed. Deletion of yeast *SDH2* is therefore superior to particular missense mutations as a model of human familial PGL predisposition. We studied an *S. cerevisiae* model of loss of function of *SDH2* (mammalian *SDHB*) for evidence of increased oxidative stress and/or succinate accumulation associated with inhibition of αKG-dependent enzymes. Individuals who inherit a heterozygous mutation in *SDHB*, *SDHC* or *SDHD* are predisposed to familial PGL by subsequent loss of heterozygosity in neuroendocrine cells (3,4,28,29). It is counter-intuitive that loss of SDH, an enzyme that contributes to energy production, leads to neoplastic transformation rather than cell death. However, it has been observed that most primary and metastatic human cancers exhibit features of the classic 'Warburg effect', showing significantly increased glucose uptake and metabolism in the presence of oxygen, with steady or decreasing oxidative phosphorylation (30,31). In fact, there is a positive correlation between levels of glycolysis in hypoxic tumors and their invasiveness and metastasis (31–33). Furthermore, many tumors carry mtDNA mutations that compromise oxidative phosphorylation, requiring tumors to survive on ATP derived from glycolysis (34–37). *S. cerevisiae* is a eukaryotic model organism that preferentially uses fermentation for ATP production. In this regard, an *sdh2*Δ yeast strain provides a relevant model of a familial PGL cancer cell that has impaired SDH function and depends upon glycolysis.

It has been hypothesized that *SDH* mutations result in ROS generation by disrupting proper electron flow (29,38,39). We hypothesized that yeast lacking the Sdh2 subunit continue to produce a catalytically active, but uncoupled Sdh1 subunit that donates electrons improperly to oxygen or water to produce ROS. A previous report suggested loss or mislocalization of the Sdh1 subunit when the *SDH2* gene is disrupted (40). However, we provide western blot and microscopic evidence for a stable Sdh1 subunit localized to the mitochondria in *sdh2*Δ cells. This result is reminiscent of observations in *SDHB*- and *SDHD*-linked PGL tumors that have lost SDHB expression but display enhanced SDHA abundance (41). A 3-fold increase in superoxide production is observed in *sdh2*Δ cells, though the origin of ROS is unclear. Preliminary data suggest that the *SOD2* gene encoding mitochondrial SOD is expressed at reduced levels in *sdh2*Δ cells, perhaps contributing to an increase in superoxide. Our data suggest that Sdh1 subunits are not catalytically active in the absence of Sdh2. In fact, we found that ROS levels are higher in *sdh1*Δ cells than in *sdh2*Δ cells.

ROS have been proposed to play a role in cellular transformation by tumorigenic mutagenesis (29,38,39). Previous reports correlating specific SDH point mutations with ROS generation have shown that *SDHC* missense mutations in certain models can lead to increased superoxide production, oxidative stress and genomic instability (6,8,42). Partial knockdown of SDHD by RNAi in rat pheochromocytoma (PC12) cells resulted in superoxide generation, whereas *SDHD* knockdown in human embryonic kidney (HEK293) cells did not (9,11). We found no evidence that superoxide generated in *sdh2*Δ cells activates oxidative stress signaling via yAP-1. However, we report here that *sdh2*Δ cells show a mild sensitivity to hydrogen peroxide that can be overcome by antioxidant treatment in a manner comparable to an *sod1*Δ mutant (43,44).

Previous reports indicate a dramatic increase in nuclear DNA mutation rate in *sod1*Δ cells that is not seen in *sdh2*Δ cells (18). In contrast, we report here that neither *sod1*Δ nor

*sdh2*Δ cells show detectable mtDNA damage in a PCR assay. Despite this, oxidized proteins accumulate in *sdh2*Δ cells. Interestingly, *sdh1*Δ cells that produce slightly more superoxide than *sdh2*Δ cells show less signs of oxidative stress. Our results demonstrate a superoxide increase in *sdh2*Δ cells that results in hypersensitivity to hydrogen peroxide and increased protein damage. These effects are comparable to those observed in *sod1Δ* and *sod2Δ* cells. These results therefore do not exclude a possible role for ROS in SDH mutants in PGL tumorigenesis.

The succinate accumulation hypothesis suggests a different mechanism for *SDH* mutations in familial PGL, though ROS and succinate accumulation hypotheses are not mutually exclusive (Fig. 1B). Mutations in *SDHB*, *SDHC* or *SDHD* may result in loss of SDH activity and a consequent accumulation of the substrate, succinate, which has the potential to inhibit αKG-dependent enzymes that normally produce succinate as a byproduct. The focus of the succinate accumulation hypothesis has been on two αKG-dependent enzymes, EglN1 and EglN3. It has been shown that SDHD knockdown using RNAi in HEK293 cells results in succinate-mediated inhibition of EglN1, an αKG-dependent prolyl hydroxylase that regulates HIF-α stability (11). There is also evidence that SDHD inhibition in PC12 cells results in succinate-mediated inhibition of EglN3, another αKG-dependent enzyme thought to play a role in c-Jun-dependent apoptosis (9).

Although HIF-1α dysregulation by succinate inhibition of EglN1 suggests an obvious mechanism in hereditary PGL, some discrepancies have been noted (9). HIF-1α acts as an oxygen sensor that is constitutively degraded by VHL under normoxic conditions. VHL is an E3 ubiquitin ligase that recognizes a HIF1-α hydroxylated proline residue, a modification catalyzed by EglN1. Mutations in VHL, a factor upstream of EglN1 in HIF-1α regulation, predispose individuals to hemangioblastoma, clear cell renal carcinoma and PHEO, presumably by inappropriate stabilization of HIF-1α. Interestingly though, PHEO development is dependent on the type of VHL mutation. For instance, VHL mutations that pose a high risk for PHEO such as L188V appear normal with respect to HIF regulation (45,46). Additionally, VHL null mutations pose a low risk of PHEO versus VHL missense mutations that pose a high risk of PHEO (47). Further, biallelic inactivation of VHL is rarely seen in PHEO compared with its more classic tumor suppressor role in hemangioblastoma and clear cell renal carcinoma (48). These results imply that complete loss of VHL function would cause HIF-1α stabilization but pose little threat of PGL (9).

Our studies corroborate and extend previous reports that loss of SDH function results in succinate accumulation with inhibition of αKG-dependent enzymes. Succinate accumulates 8-fold in *sdh2*Δ yeast cells relative to WT cells and we show for the first time that this succinate accumulation results in inhibition of the αKG-dependent enzyme Jlp1. This sulfur-scavenging enzyme enables yeast to utilize sulfonate esters as their sole sulfur source (24). Jlp1 is inhibited not only by succinate accumulation in *sdh2*Δ cells, but also by exogenous succinate in WT cells. Remarkably, succinate inhibition of Jlp1 can be overcome by treatment with exogenous αKG. There is no evidence to suggest that yeast sulfur metabolism has a correlate in mammalian tumorigenesis. Nonetheless, these results substantiate that inhibition of αKG-dependent enzymes by succinate accumulation is a general consequence of SDH loss.

It remains unclear which αKG-dependent enzymes are the relevant targets for succinate inhibition in the etiology of familial PGL. Our work provides evidence that targets are not limited to EglN1 and EglN3. JHDMs utilize an αKG-dependent enzyme mechanism and have recently been identified and characterized in humans and *S. cerevisiae* (13,14). Including Jhd1, a total of five JmjC domain enzymes exist in *S. cerevisiae*, with four demonstrated to be functional histone demethylases (14). We hypothesized that Jhd1, a yeast JHDM that specifically demethylates H3-K36me2 could be inhibited by the succinate accumulated in *sdh2*Δ cells, corresponding to the phenotype of *jhd1*Δ yeast. Indeed, we observed increased levels of H3-K36me2 in both *sdh2*Δ and *jhd1*Δ cells. Furthermore, we demonstrated that extracellular succinate and αKG influence the level of H3-K36me2. A previous transcription profiling study of *sdh2*Δ yeast indicated that expression of 58 genes changed by at least 2.5-fold relative to WT (49). Intriguingly, seven of these genes encode protein kinases, signaling components and transcription factors not obviously related to regulation of metabolism.

To demonstrate the potential for succinate inhibition of human JHDMs, we measured the histone demethylase activity of a human JHDM, JMJD2D, under varying conditions *in vitro*. We show that a range of succinate concentrations inhibits JMJD2D demethylation of H3-K9me3 and that this effect could be reversed with increasing concentrations of αKG. We also found that exogenous succinate can cause human JMJD2D inhibition in living cells. The implications of succinate inhibition on histone demethylases are profound. It will prove challenging to determine what demethylases are most susceptible to succinate poisoning in a neuroectodermal environment relevant to PGL development.

Inhibition of the H3K36me2 demethylase by elevated levels of succinate has crucial implications for the potential role of epigenetics in familial PGL tumorigenesis. The post-translational modification of histone tails profoundly affects chromatin structure and function (50). Histone methylation occurring on lysine or arginine residues of H3 and H4 tail domains can target chromatin for activation or repression (51,52). The yeast H3-K36 methylase, Set2, mediates transcriptional repression (53,54). Conversely, it has been demonstrated that the yeast H3-K36 demethylase, Jhd1, acts as a transcriptional activator (55). We hypothesize that succinate-mediated inhibition of the mammalian JHDMs could play a role in cellular transformation by misregulation of genes that are responsible for DNA repair, growth inhibition or induction of apoptosis. Experiments to assess the growth-control phenotype upon histone demethylase inhibition are complicated by the presence of four such functional enzymes in *S. cerevisiae* (14). Future efforts to identify JHDMs inhibited by succinate and the genes affected by their inhibition will provide insight into the role of succinate inhibition of the mammalian JHDMs and its impact on development of familial PGL. Indeed, specific histone methylation marks are required for DNA transcriptional regulation and DNA repair (56). Deregulation of histone demethylases in cancer etiology is an import-

ant topic for future research. The potential deregulation of epigenetic gene control in PGL is provocative in light of the imprinted pattern of inheritance of *SDHD* mutations (1,3).

Not only has succinate accumulation been reported here in an *in vivo* yeast model of SDHB loss and in *in vitro* experiments that target SDHD with siRNA (9,11), but also succinate accumulation has been reported in at least two patients with SDHB mutant PGL tumors. Both patients carried an *SDHB* mutation in the iron-sulfur cluster region of the gene (I127S) and lost the second copy of *SDHB* in PGL tumors (57). A 10-fold increase in tumor succinate was reported, comparable to the 8-fold succinate increase we measured in *sdh2*Δ yeast cells relative to WT cells. These findings substantiate the potential role of accumulated succinate in hereditary PGL tumors.

As highlighted by a recent report of an anti-angiogenic prolyl hydroxylase of the same αKG-dependent enzyme superfamily (12), other candidate αKG-dependent enzymes also remain to be explored as possible links between succinate accumulation and oncogenesis. Our work points to the potential significance of such enzymes in the etiology of familial PGL.

MATERIALS AND METHODS

Strains, media and culture conditions

The *sdh1*Δ, *sdh2*Δ, *sod1*Δ, *jhd1*Δ and *set2*Δ strains and their parental strain BY4741 (*MAT*a *his31 leu20 met150 ura30*), as well as *sdh2*Δ and *jlp1*Δ strains, and their parental strain BY4742 (*MAT*a *ura3 leu2 his3 lys2*) were the kind gifts of D. Katzmann. Sdh1 was C-terminally tagged with GFP in WT and *sdh2*Δ yeast using the pFA6a-GFP(S65T)-HIS3MX6 module as described (58). Yeast strains were grown in YPD (1% yeast extract, 2% peptone, 2% dextrose) medium (BD Biosciences), YPGal (1% yeast extract, 2% peptone, 2% galactose) medium, YPGlycerol (1% yeast extract, 2% peptone, 3% glycerol) or YPE (1% yeast extract, 2% peptone, 2% ethanol). Yeast cells containing *lacZ* reporter plasmids were grown on uracil dropout medium containing dextrose. Nutritional assays with different sulfur sources were performed in minimal medium devoid of sulfur as described (59), supplemented with isethionate (20 μM) or ammonium sulfate (250 mM) as indicated. Preparative cultures were grown aerobically with shaking (250 r.p.m.) at 30°C. Growth was monitored by measuring the culture optical density at 600 nm (OD_{600}).

β-Galactosidase assays

Plasmid pJ1291 (original name pCEP14) was the generous gift of S. Moye-Rowley. This is a *URA3*-containing CEN plasmid (pSEYC102 backbone) that carries four AP1 binding sites upstream of the CYC1 promoter fused to *lacZ*. Yeast strains were transformed using a standard lithium acetate transformation protocol (60). Cells were incubated with or without 100 μM H_2O_2 for 90 min at 30°C. β-Galactosidase assays were conducted using the substrate *o*-nitrophenyl-D-galactopyranoside as described (61). Data representing triplicate experiments are expressed as activities in Miller units.

Yeast whole cell extraction and western blot analysis

Transformants expressing Sdh1-GFP were grown in YPGal and harvested at mid-log phase (OD_{600}=0.8–1.0). Equal samples (five OD_{600}) were precipitated with trichloroacetic acid (10% final volume) and broken by sonication and glass bead lysis in sample buffer (62.5 mM Tris–HCl, pH 6.8, 2% SDS, 5% β-mercaptoethanol, 10% glycerol, 0.01% bromophenol blue). After clarification, supernatants were collected and assayed immediately or stored at −80°C. Equal volumes of yeast extract were electrophoresed through denaturing 10% bis-Tris polyacrylamide gels and transferred to nitrocellulose membrane. Equal loading was demonstrated by Ponceau S stain (Sigma). After blocking (5% non-fat dry milk, Tris-buffered saline, 1% Tween-20), membranes were probed with polyclonal anti-GFP (BD Biosciences) at a dilution of 1:1000. Horseradish peroxidase-conjugated anti-mouse secondary antibody (Pierce) and an ECL kit (Amersham) were used to detect immunoreactive proteins.

Yeast nuclei preparation and western blot analysis

Yeast nuclei were prepared from overnight cultures grown in YPGal that were at 1.5–2.0 OD/ml as described (62). Cells were grown in the absence or presence of 50 mM succinate and/or 1 mM αKG, where indicated. Nuclear protein was quantitated by Bradford assay (BioRad). Protein samples (40 μg) were sonicated briefly and boiled for 5 min and clarified before electrophoresis through a denaturing 10% bis-Tris polyacrylamide gel and transferred to nitrocellulose membrane. After blocking, membranes were probed with polyclonal anti-H3-K36me2 antibody (Upstate, #07–274) at a dilution of 1:2000 or polyclonal anti-H3 antibody (generous gift of Z. Zhang). Horseradish peroxidase-conjugated anti-rabbit secondary antibody (Zymed) and an ECL Plus kit (Amersham) were used to detect immunoreactive proteins.

Fluorescence microscopy

Yeast transformants expressing Sdh1-GFP were grown overnight at 26°C, diluted and grown to early exponential phase (OD_{600}=0.4–0.6). Cells were pelleted and resuspended in yeast nitrogen medium without tryptophan (YNB-Trp), containing 10 nM tetramethylrhodamine (the generous gift of C. McMurray). After incubation for 10 min at 25°C, cells were pelleted and resuspended in YNB-Trp. Microscopy was performed on living cells using a fluorescence microscope (Nikon) fitted with FITC and rhodamine filters and a digital camera (Coolsnap HQ; Photometrix). Images were deconvolved using Delta Vision software (Applied Precision, Inc.) and processed with Adobe Photoshop 5.0 software.

Superoxide sensitivity

Yeast growth was assessed on solid YPGal medium containing a H_2O_2 gradient of up to 18 mM or on YPE containing an antioxidant gradient up to 1× (antioxidant supplement A1345, Sigma). Yeast (2 OD_{600}) were pelleted from cultures grown to saturation in YPGal, washed once with sterile water, and resuspended in 1 mL sterile water. Yeast were diluted by a

factor of 10^3 and 3.5 μL of dilution was spotted on solid medium.

Isolation of mitochondria and enzyme assays

Yeast cells grown to stationary phase in YPGal were harvested by centrifugation and lysed by vortexing with 0.5-mm acid-washed glass beads in mannitol buffer (210 mM mannitol, 70 mM sucrose, 5 mM Tris–HCl pH 7.5, 5 mM EDTA) using three 5 min pulses interspersed with 3 min cooling periods on ice. Complete protease inhibitor mixture tablets (Roche Diagnostics) were added prior to cell lysis. Mitochondria were isolated by differential centrifugation (22). The lysate was subjected to 5 min centrifugation in a benchtop microfuge at 20*g*, then the resulting supernatant was subjected to centrifugation at 6400*g* for 20 min and the pellet was resuspended in cold mannitol buffer at 4°C. SDH activity was measured spectrophotometrically at 30°C as the malonate-sensitive reduction of 2,6-dichlorophenolindophenol (DCPIP, 50 mM) at A_{600} in the presence of 4 mM sodium azide, 20 mM succinate and with or without 14 mM malonate (40). NADH dehydrogenase, complex II+III and complex IV activities were measured spectrophotometrically at 37°C as described (63).

Krebs cycle metabolites

Yeast whole cell extracts were prepared by glass bead lysis from cultures grown to mid-log phase in YPGal. Organic acids were assayed as described (64). Briefly, yeast extracts were acidified with HCl (0.5 M final concentration), then extracted with ethyl acetate. After evaporation, the dry residue was silyated with *N*,*O*-bis (trismethylsilyl) trifluoroacetamide containing 1% trimethylchlorosilane and analyzed using a Hewlett Packard 6890/5973 or 6890/5972 capillary GC/MS instrument with MSD 5973 or 5972 detector.

Detection of superoxide radicals

DHE (Molecular Probes) was added to early exponential phase cultures of WT, *sdh1*Δ or *sdh2*Δ cells. Cultures were then grown in YPGal medium to A_{600}=0.4–0.5. As a control, WT cells (BY4741) were treated with 250 μg/ml antimycin A for 1 h before assay. Cultures were incubated in 50 mM Tris pH 7.6 containing 150 mM DHE for 30 min and washed once with Tris buffer before analysis by fluorometry (excitation/emission: 485/595 nm) or microscopy (excitation/emission: 580/630 nm).

Detection of protein oxidation

Aldehyde oxidation products were immunologically detected in proteins using an OxyBlot kit (Intergen). Equal amounts of yeast extract were treated with 2,4-dinitrophenylhydrazine to derivatize carbonyl groups to 2,4-dinitrophenylhydrazone (DNP-hydrazone) as described by the manufacturer. Proteins were then separated on a 10% denaturing bis–Tris polyacrylamide gel and transferred to nitrocellulose. The membrane was probed with a primary antibody specific for DNP-hydrazone protein derivatives, followed by a secondary antibody conjugated to horseradish peroxidase. Modified proteins were detected with ECL reagents (Amersham Pharmacia) and imaged by exposure to Kodak BioMax XAR film.

Dna isolation and damage analysis by qpcr

DNA was extracted from yeast strains (MasterPure Yeast DNA purification kit, Epicentre). Control DNA was harvested from WT yeast incubated with 0.5, 1 or 5 mM H_2O_2 for 1 h at 30°C. Mitochondrial DNA (mtDNA) was analyzed by QPCR assay of 298 bp and 6.9 kbp mtDNA regions near the *COX1* gene as described in (15). Results reflect the mean of three sets of PCR amplifications for each target gene.

Preparation of GST fusion proteins

Glutathione *S*-transferase (GST) fusion proteins of JHDM3/JMJD2D and its H192A mutant were produced in *Escherichia coli* and purified on glutathione-agarose beads according to standard procedures (65). After elution with 20 mM glutathione/100 mM Tris pH 8, GST fusion proteins were dialyzed against 10 mM HEPES pH 7.4, 50 mM NaCl, 1 mM DTT, 0.2 mM PMSF, 10% glycerol and then stored at −80°C after freezing in liquid nitrogen.

Histone extracts for *in vivo* histone demethylase activity

293T cells were grown in 6 cm dishes coated with poly-L-lysine and transiently transfected by the calcium phosphate coprecipitation method (66,67) utilizing 9 μg pBluescript KS^+ and either 0.3 μg pEV3S vector or 0.3 μg (or 0.9 μg) Flag-JMJD2D expression vector (68). Twelve hours after removal of the precipitate, cells were treated with 100 mM DMS where indicated and incubated for another 24 h at 37°C in a humidified atmosphere containing 10% CO_2 as described before (69). Then, cells were lysed in 75–150 μl of 10 mM Tris, 30 mM $Na_4P_2O_7$ pH 7.1, 200 mM NaCl, 50 mM NaF, 0.5 mM Na_3VO_4, 1% Triton X-100, 1 mM dithiothreitol, 20 μg/ml leupeptin, 4 μg/ml aprotinin, 2 μg/ml pepstatin A, 1 mM phenylmethylsulfonyl fluoride. An equal volume of 2× Laemmli sample buffer was added after 30 min and the extracts were boiled for 10 min. Debris was removed by centrifugation and supernatants employed for Western blotting as described before (70).

Measurement of *in vitro* histone demethylase activity

Histone demethylase activity was assessed in fresh assay buffer (50 mM HEPES, 50 mM NaCl, 50 mM KCl, 2 mM ascorbate, 0.2 mM $Fe(NH_4)_2SO_4$) and a range of αKG (0.01–5 mM) and succinate (0–10 mM) concentrations. One microgram of GST fusion protein was incubated with 1 μg histones (USB) in a 15 μl reaction at 37°C for 1.5 h. Reactions were quenched on ice, treated with LDS sample buffer (Invitrogen) and 0.5 μl BME and boiled for 5 min. Samples were loaded on a denaturing 12% bis-Tris polyacrylamide gel and transferred to nitrocellulose (as described above). The top portion of the membrane (proteins greater than 30 kDa) was removed and stained with Coomassie blue dye to demonstrate equal loading of JHDM3 (JMJD2D). The lower portion of the membrane was blocked with 5% milk/TBST and probed with

anti-H3-K9me3 antibody (Abcam, ab8898) at a dilution of 1:1000. Horseradish peroxidase-conjugated anti-rabbit secondary antibody (Zymed) and an ECL kit (Pierce) were used to detect immunoreactive proteins.

SUPPLEMENTARY MATERIAL

Supplementary Material is available at HMG Online.

ACKNOWLEDGEMENTS

We thank P. Rinaldo and D. Hinrichs, S. Hahn, S. Hartman and K. Kramer from the Biochemical Genetics Core at the Mayo Clinic College of Medicine for measurement of TCA cycle metabolites and for initial enzyme assays. We appreciate advice, yeast strains, reagents and technical assistance from D. Katzmann, A. Oestreich, J. Payne (Mayo) and K. Kizer (University of North Carolina School of Medicine, Chapel Hill). The technical advice and support of E. Arriaga and D. Li (University of Minnesota) and M. Ramirez-Alvarado (Mayo) were of value in DHE methodology. C. McMurray and Z. Zhang (Mayo) and S. Moye-Rowley (University of Iowa) provided essential materials. We appreciate the insightful comments and encouragement of our colleagues G. Isaya and W. Young.

Conflict of Interest statement. None declared.

FUNDING

This work was supported by the Mayo Foundation and a grant from the Fraternal Order of Eagles. Funding for open access charge: the Mayo Foundation.

REFERENCES

1. Baysal, B.E., Rubinstein, W.S. and Taschner, P.E. (2001) Phenotypic dichotomy in mitochondrial complex II genetic disorders. *J. Mol. Med.*, **79**, 495–503.
2. Astuti, D., Latif, F., Dallol, A., Dahia, P.L., Douglas, F., George, E., Skoldberg, F., Husebye, E.S., Eng, C. and Maher, E.R. (2001) Gene mutations in the succinate dehydrogenase subunit SDHB cause susceptibility to familial pheochromocytoma and to familial paraganglioma. *Am. J. Hum. Genet.*, **69**, 49–54.
3. Baysal, B.E., Ferrell, R.E., Willett-Brozick, J.E., Lawrence, E.C., Myssiorek, D., Bosch, A., van der Mey, A., Taschner, P.E., Rubinstein, W.S., Myers, E.N. *et al.* (2000) Mutations in SDHD, a mitochondrial complex II gene, in hereditary paraganglioma. *Science*, **287**, 848–851.
4. Niemann, S. and Muller, U. (2000) Mutations in SDHC cause autosomal dominant paraganglioma, type 3. *Nat. Genet.*, **26**, 268–270.
5. Guo, J. and Lemire, B.D. (2003) The ubiquinone-binding site of the *Saccharomyces cerevisiae* succinate-ubiquinone oxidoreductase is a source of superoxide. *J. Biol. Chem.*, **278**, 47629–47635.
6. Ishii, N., Fujii, M., Hartman, P.S., Tsuda, M., Yasuda, K., Senoo-Matsuda, N., Yanase, S., Ayusawa, D. and Suzuki, K. (1998) A mutation in succinate dehydrogenase cytochrome *b* causes oxidative stress and ageing in nematodes. *Nature*, **394**, 694–697.
7. Oostveen, F.G., Au, H.C., Meijer, P.J. and Scheffler, I.E. (1995) A Chinese hamster mutant cell line with a defect in the integral membrane protein CII-3 of complex II of the mitochondrial electron transport chain. *J. Biol. Chem.*, **270**, 26104–26108.
8. Ishii, T., Yasuda, K., Akatsuka, A., Hino, O., Hartman, P.S. and Ishii, N. (2005) A mutation in the SDHC gene of complex II increases oxidative stress, resulting in apoptosis and tumorigenesis. *Cancer Res.*, **65**, 203–209.
9. Lee, S., Nakamura, E., Yang, H., Wei, W., Linggi, M.S., Sajan, M.P., Farese, R.V., Freeman, R.S., Carter, B.D., Kaelin, W.G., Jr *et al.* (2005) Neuronal apoptosis linked to EglN3 prolyl hydroxylase and familial pheochromocytoma genes: developmental culling and cancer. *Cancer Cell*, **8**, 155–167.
10. Maxwell, P.H. (2005) A common pathway for genetic events leading to pheochromocytoma. *Cancer Cell*, **8**, 91–93.
11. Selak, M.A., Armour, S.M., MacKenzie, E.D., Boulahbel, H., Watson, D.G., Mansfield, K.D., Pan, Y., Simon, M.C., Thompson, C.B. and Gottlieb, E. (2005) Succinate links TCA cycle dysfunction to oncogenesis by inhibiting HIF-alpha prolyl hydroxylase. *Cancer Cell*, **7**, 77–85.
12. Teodoro, J.G., Parker, A.E., Zhu, X. and Green, M.R. (2006) p53-mediated inhibition of angiogenesis through up-regulation of a collagen prolyl hydroxylase. *Science*, **313**, 968–971.
13. Klose, R.J., Kallin, E.M. and Zhang, Y. (2006) JmjC-domain-containing proteins and histone demethylation. *Nat. Rev. Genet.*, **7**, 715–727.
14. Tu, S., Bulloch, E.M., Yang, L., Ren, C., Huang, W.C., Hsu, P.H., Chen, C.H., Liao, C.L., Yu, H.M., Lo, W.S. *et al.* (2007) Identification of histone demethylases in *Saccharomyces cerevisiae*. *J. Biol. Chem.*, **282**, 14262–14271.
15. Rasmussen, A.K., Chatterjee, A., Rasmussen, L.J. and Singh, K.K. (2003) Mitochondria-mediated nuclear mutator phenotype in *Saccharomyces cerevisiae*. *Nucleic Acids Res.*, **31**, 3909–3917.
16. O'Brien, K.M., Dirmeier, R., Engle, M. and Poyton, R.O. (2004) Mitochondrial protein oxidation in yeast mutants lacking manganese-(MnSOD) or copper- and zinc-containing superoxide dismutase (CuZnSOD): evidence that MnSOD and CuZnSOD have both unique and overlapping functions in protecting mitochondrial proteins from oxidative damage. *J. Biol. Chem.*, **279**, 51817–51827.
17. Wardman, P. and Candeias, L.P. (1996) Fenton chemistry: an introduction. *Radiat. Res.*, **145**, 523–531.
18. Huang, M.E., Rio, A.G., Nicolas, A. and Kolodner, R.D. (2003) A genomewide screen in *Saccharomyces cerevisiae* for genes that suppress the accumulation of mutations. *Proc. Natl Acad. Sci. U.S.A.*, **100**, 11529–11534.
19. Woodruff, R.C., Phillips, J.P. and Hilliker, A.J. (2004) Increased spontaneous DNA damage in Cu/Zn superoxide dismutase (SOD1) deficient *Drosophila*. *Genome*, **47**, 1029–1035.
20. Gralla, E.B. and Valentine, J.S. (1991) Null mutants of *Saccharomyces cerevisiae* Cu,Zn superoxide dismutase: characterization and spontaneous mutation rates. *J. Bacteriol.*, **173**, 5918–5920.
21. Chary, P., Dillon, D., Schroeder, A.L. and Natvig, D.O. (1994) Superoxide dismutase (sod-1) null mutants of Neurospora crassa: oxidative stress sensitivity, spontaneous mutation rate and response to mutagens. *Genetics*, **137**, 723–730.
22. Karthikeyan, G., Santos, J.H., Graziewicz, M.A., Copeland, W.C., Isaya, G., Van Houten, B. and Resnick, M.A. (2003) Reduction in frataxin causes progressive accumulation of mitochondrial damage. *Hum. Mol. Genet.*, **12**, 3331–3342.
23. Kuge, S., Jones, N. and Nomoto, A. (1997) Regulation of yAP-1 nuclear localization in response to oxidative stress. *EMBO J.*, **16**, 1710–1720.
24. Hogan, D.A., Auchtung, T.A. and Hausinger, R.P. (1999) Cloning and characterization of a sulfonate/alpha-ketoglutarate dioxygenase from *Saccharomyces cerevisiae*. *J. Bacteriol.*, **181**, 5876–5879.
25. Hausinger, R.P. (2004) FeII/alpha-ketoglutarate-dependent hydroxylases and related enzymes. *Crit. Rev. Biochem. Mol. Biol.*, **39**, 21–68.
26. Kizer, K.O., Phatnani, H.P., Shibata, Y., Hall, H., Greenleaf, A.L. and Strahl, B.D. (2005) A novel domain in Set2 mediates RNA polymerase II interaction and couples histone H3 K36 methylation with transcript elongation. *Mol. Cell. Biol.*, **25**, 3305–3316.
27. Tsukada, Y., Fang, J., Erdjument-Bromage, H., Warren, M.E., Borchers, C.H., Tempst, P. and Zhang, Y. (2006) Histone demethylation by a family of JmjC domain-containing proteins. *Nature*, **439**, 811–816.
28. Gimenez-Roqueplo, A.P., Favier, J., Rustin, P., Mourad, J.J., Plouin, P.F., Corvol, P., Rotig, A. and Jeunemaitre, X. (2001) The R22X mutation of the SDHD gene in hereditary paraganglioma abolishes the enzymatic activity of complex II in the mitochondrial respiratory chain and activates the hypoxia pathway. *Am. J. Hum. Genet.*, **69**, 1186–1197.
29. Eng, C., Kiuru, M., Fernandez, M.J. and Aaltonen, L.A. (2003) A role for mitochondrial enzymes in inherited neoplasia and beyond. *Nat. Rev. Cancer*, **3**, 193–202.

30. Warburg, O. (1956) On the origin of cancer cells. *Science*, **123**, 309–314.
31. Gatenby, R.A. and Gillies, R.J. (2004) Why do cancers have high aerobic glycolysis? *Nat. Rev. Cancer*, **4**, 891–899.
32. He, X., Brenchley, P.E., Jayson, G.C., Hampson, L., Davies, J. and Hampson, I.N. (2004) Hypoxia increases heparanase-dependent tumor cell invasion, which can be inhibited by antiheparanase antibodies. *Cancer Res.*, **64**, 3928–3933.
33. Yoon, S.O., Shin, S. and Mercurio, A.M. (2005) Hypoxia stimulates carcinoma invasion by stabilizing microtubules and promoting the Rab11 trafficking of the alpha6beta4 integrin. *Cancer Res.*, **65**, 2761–2769.
34. Carew, J.S. and Huang, P. (2002) Mitochondrial defects in cancer. *Mol. Cancer*, **1**, 9.
35. Hibi, K., Nakayama, H., Yamazaki, T., Takase, T., Taguchi, M., Kasai, Y., Ito, K., Akiyama, S. and Nakao, A. (2001) Detection of mitochondrial DNA alterations in primary tumors and corresponding serum of colorectal cancer patients. *Int. J. Cancer*, **94**, 429–431.
36. Lee, H.C., Yin, P.H., Lin, J.C., Wu, C.C., Chen, C.Y., Wu, C.W., Chi, C.W., Tam, T.N. and Wei, Y.H. (2005) Mitochondrial Genome Instability and mtDNA Depletion in Human Cancers. *Ann. NY Acad. Sci.*, **1042**, 109–122.
37. Polyak, K., Li, Y., Zhu, H., Lengauer, C., Willson, J.K., Markowitz, S.D., Trush, M.A., Kinzler, K.W. and Vogelstein, B. (1998) Somatic mutations of the mitochondrial genome in human colorectal tumours. *Nat. Genet.*, **20**, 291–293.
38. Baysal, B.E., Willett-Brozick, J.E., Filho, P.A., Lawrence, E.C., Myers, E.N. and Ferrell, R.E. (2004) An Alu-mediated partial SDHC deletion causes familial and sporadic paraganglioma. *J. Med. Genet.*, **41**, 703–709.
39. Storz, P. (2005) Reactive oxygen species in tumor progression. *Front. Biosci.*, **10**, 1881–1896.
40. Schmidt, D.M., Saghbini, M. and Scheffler, I.E. (1992) The C-terminus of the succinate dehydrogenase IP peptide of *Saccharomyces cerevisiae* is significant for assembly of complex II. *Biochemistry*, **31**, 8442–8448.
41. Douwes Dekker, P.B., Hogendoorn, P.C., Kuipers-Dijkshoorn, N., Prins, F.A., van Duinen, S.G., Taschner, P.E., van der Mey, A.G. and Cornelisse, C.J. (2003) SDHD mutations in head and neck paragangliomas result in destabilization of complex II in the mitochondrial respiratory chain with loss of enzymatic activity and abnormal mitochondrial morphology. *J. Pathol.*, **201**, 480–486.
42. Albayrak, T., Scherhammer, V., Schoenfeld, N., Braziulis, E., Mund, T., Bauer, M.K., Scheffler, I.E. and Grimm, S. (2003) The tumor suppressor cybL, a component of the respiratory chain, mediates apoptosis induction. *Mol. Biol. Cell*, **14**, 3082–3096.
43. Koziol, S., Zagulski, M., Bilinski, T. and Bartosz, G. (2005) Antioxidants protect the yeast *Saccharomyces cerevisiae* against hypertonic stress. *Free Radic. Res.*, **39**, 365–371.
44. Carter, C.D., Kitchen, L.E., Au, W.C., Babic, C.M. and Basrai, M.A. (2005) Loss of SOD1 and LYS7 sensitizes *Saccharomyces cerevisiae* to hydroxyurea and DNA damage agents and downregulates MEC1 pathway effectors. *Mol. Cell. Biol.*, **25**, 10273–10285.
45. Clifford, S.C., Cockman, M.E., Smallwood, A.C., Mole, D.R., Woodward, E.R., Maxwell, P.H., Ratcliffe, P.J. and Maher, E.R. (2001) Contrasting effects on HIF-1α regulation by disease-causing pVHL mutations correlate with patterns of tumourigenesis in von Hippel-Lindau disease. *Hum. Mol. Genet.*, **10**, 1029–1038.
46. Hoffman, M.A., Ohh, M., Yang, H., Klco, J.M., Ivan, M. and Kaelin, W.G., Jr. (2001) von Hippel-Lindau protein mutants linked to type 2C VHL disease preserve the ability to downregulate HIF. *Hum. Mol. Genet.*, **10**, 1019–1027.
47. Zbar, B., Kishida, T., Chen, F., Schmidt, L., Maher, E.R., Richards, F.M., Crossey, P.A., Webster, A.R., Affara, N.A., Ferguson-Smith, M.A. *et al.* (1996) Germline mutations in the Von Hippel-Lindau disease (VHL) gene in families from North America, Europe, and Japan. *Hum. Mutat.*, **8**, 348–357.
48. Kim, W. and Kaelin, W.G., Jr. (2003) The von Hippel–Lindau tumor suppressor protein: new insights into oxygen sensing and cancer. *Curr. Opin. Genet. Dev.*, **13**, 55–60.
49. McCammon, M.T., Epstein, C.B., Przybyla-Zawislak, B., McAlister-Henn, L. and Butow, R.A. (2003) Global transcription analysis of Krebs tricarboxylic acid cycle mutants reveals an alternating pattern of gene expression and effects on hypoxic and oxidative genes. *Mol. Biol. Cell*, **14**, 958–972.
50. Grant, P.A. (2001) A tale of histone modifications. *Genome Biol.*, **2**, 1–6.
51. Zhang, Y. and Reinberg, D. (2001) Transcription regulation by histone methylation: interplay between different covalent modifications of the core histone tails. *Genes Dev.*, **15**, 2343–2360.
52. Kouzarides, T. (2002) Histone methylation in transcriptional control. *Curr. Opin. Genet. Dev.*, **12**, 198–209.
53. Strahl, B.D., Grant, P.A., Briggs, S.D., Sun, Z.W., Bone, J.R., Caldwell, J.A., Mollah, S., Cook, R.G., Shabanowitz, J., Hunt, D.F. *et al.* (2002) Set2 is a nucleosomal histone H3-selective methyltransferase that mediates transcriptional repression. *Mol. Cell. Biol.*, **22**, 1298–1306.
54. Landry, J., Sutton, A., Hesman, T., Min, J., Xu, R.M., Johnston, M. and Sternglanz, R. (2003) Set2-catalyzed methylation of histone H3 represses basal expression of GAL4 in *Saccharomyces cerevisiae*. *Mol. Cell. Biol.*, **23**, 5972–5978.
55. Titz, B., Thomas, S., Rajagopala, S.V., Chiba, T., Ito, T. and Uetz, P. (2006) Transcriptional activators in yeast. *Nucleic Acids Res.*, **34**, 955–967.
56. Shi, Y. and Whetstine, J.R. (2007) Dynamic regulation of histone lysine methylation by demethylases. *Mol. Cell*, **25**, 1–14.
57. Pollard, P.J., Briere, J.J., Alam, N.A., Barwell, J., Barclay, E., Wortham, N.C., Hunt, T., Mitchell, M., Olpin, S., Moat, S.J. *et al.* (2005) Accumulation of Krebs cycle intermediates and over-expression of HIF1alpha in tumours which result from germline FH and SDH mutations. *Hum. Mol. Genet.*, **14**, 2231–2239.
58. Longtine, M.S., McKenzie, A., III., Demarini, D.J., Shah, N.G., Wach, A., Brachat, A., Philippsen, P. and Pringle, J.R. (1998) Additional modules for versatile and economical PCR-based gene deletion and modification in *Saccharomyces cerevisiae*. *Yeast*, **14**, 953–961.
59. Cherest, H. and Surdin-Kerjan, Y. (1992) Genetic analysis of a new mutation conferring cysteine auxotrophy in *Saccharomyces cerevisiae*: updating of the sulfur metabolism pathway. *Genetics*, **130**, 51–58.
60. CLONTECH (1999) *Yeast Protocols Handbook PT3024-1*. CLONTECH, Palo Alto, CA.
61. Guarente, L. (1983) Yeast promoters and lacZ fusions designed to study expression of cloned genes in yeast. *Methods Enzymol.*, **101**, 181–191.
62. Kizer, K.O., Xiao, T. and Strahl, B.D. (2006) Accelerated nuclei preparation and methods for analysis of histone modifications in yeast. *Methods*, **40**, 296–302.
63. Kramer, K.A., Oglesbee, D., Hartman, S.J., Huey, J., Anderson, B., Magera, M.J., Matern, D., Rinaldo, P., Robinson, B.H., Cameron, J.M. *et al.* (2005) Automated spectrophotometric analysis of mitochondrial respiratory chain complex enzyme activities in cultured skin fibroblasts. *Clin. Chem.*, **51**, 2110–2116.
64. Rinaldo, P., Hahn, S. and Matern, D. (2005) Inborn errors of amino acid, organic acid, and fatty acid metabolism. In Burtis, C., Ashwood, E. and Bruns, D. (eds), *Tietz Textbook of Clinical Chemistry and Molecular Diagnostics*, 4th edn. Saunders, W.B., Philadelphia, pp. 2207–2247.
65. Janknecht, R. (2003) Regulation of the ER81 transcription factor and its coactivators by mitogen- and stress-activated protein kinase 1 (MSK1). *Oncogene*, **22**, 746–755.
66. Goueli, B.S. and Janknecht, R. (2004) Upregulation of the catalytic telomerase subunit by the transcription factor ER81 and oncogenic HER2/Neu, Ras, or Raf. *Mol. Cell. Biol.*, **24**, 25–35.
67. Janknecht, R. (1996) Analysis of the ERK-stimulated ETS transcription factor ER81. *Mol. Cell. Biol.*, **16**, 1550–1556.
68. Shin, S. and Janknecht, R. (2007) Diversity within the JMJD2 histone demethylase family. *Biochem. Biophys. Res. Commun.*, **353**, 973–977.
69. Janknecht, R., Ernst, W.H. and Nordheim, A. (1995) SAP1a is a nuclear target of signaling cascades involving ERKs. *Oncogene*, **10**, 1209–1216.
70. Papoutsopoulou, S. and Janknecht, R. (2000) Phosphorylation of ETS transcription factor ER81 in a complex with its coactivators CREB-binding protein and p300. *Mol. Cell. Biol.*, **20**, 7300–7310.